



**HAL**  
open science

## Two-dimensional versus three-dimensional constraints in hetero-epitaxy/orientation relationships

Paul Wynblatt, Dominique Chatain

► **To cite this version:**

Paul Wynblatt, Dominique Chatain. Two-dimensional versus three-dimensional constraints in hetero-epitaxy/orientation relationships. *Journal of Materials Science*, 2017, 52 (16), pp.9630 - 9639. 10.1007/s10853-017-1145-z . hal-01720666

**HAL Id: hal-01720666**

**<https://hal.science/hal-01720666>**

Submitted on 13 Apr 2018

**HAL** is a multi-disciplinary open access archive for the deposit and dissemination of scientific research documents, whether they are published or not. The documents may come from teaching and research institutions in France or abroad, or from public or private research centers.

L'archive ouverte pluridisciplinaire **HAL**, est destinée au dépôt et à la diffusion de documents scientifiques de niveau recherche, publiés ou non, émanant des établissements d'enseignement et de recherche français ou étrangers, des laboratoires publics ou privés.

# Two-dimensional versus Three-dimensional Constraints in Hetero-Epitaxy/Orientation Relationships

Paul Wynblatt<sup>1</sup>, Dominique Chatain<sup>2\*</sup>

<sup>1</sup>Department of Materials Science and Engineering, Carnegie Mellon University, Pittsburgh,  
PA 15213, USA

email: pw01@andrew.cmu.edu

<sup>2</sup>Aix-Marseille Univ, CNRS, CINAM, 13009 Marseille, France

email: chatain@cinam.univ-mrs.fr

## Abstract

Molecular Dynamics simulations have been performed to compare the orientation relationships (ORs) that develop between Ag films/particles equilibrated with Ni, depending on whether the Ag is subjected to three-dimensional (3-D) confinement by being embedded in Ni, or to 2-D confinement by equilibration with a Ni substrate. Previous results of both simulations and experiments have shown that Ag films equilibrated with planar Ni substrates display a large number of different ORs; in particular, Ag equilibrated on Ni{100} displays an OR of Ag{111}<110> // Ni{100}<110>, often referred to as an oct-cube OR. Here it is shown that a Ag particle embedded in Ni displays an OR of Ag{111}<110> // Ni{111}<110>, i.e. a cube-on-cube OR. It has also been shown that as the confinement of a Ag particle is gradually increased from 2-D to 3-D, by equilibrating a Ag particle on Ni(100) substrates with progressively deeper dimples, a transition in OR occurs from oct-cube to cube-on-cube. This result contradicts the conventional notion which supposes that the ORs displayed in the presence of 3-D confinement (e.g. during phase transformations) will also tend to be displayed in epitaxy on a substrate.

**Keywords:** orientation relationship, interface anisotropy, particle confinement, lattice mismatch, surface and interface structure

## INTRODUCTION

The orientation relationship (OR)/hetero-epitaxy that is manifested when one crystalline material grows either *on* or *within* another may depend on the dimensionality of the template on which growth takes place. For example, in phase transformations the OR that develops is one that minimizes the energy of the new phase under conditions where it is surrounded in 3-dimensions (3-D) by the parent phase, whereas in film epitaxy the OR of the film is constrained to adapt to a "flat" 2-D substrate of arbitrary but specific orientation. Thus the resultant OR in hetero-epitaxy of one phase on a flat surface of another phase does not necessarily need to duplicate the OR which arises in phase transformations. In this paper, we investigate the dependence of the OR on the dimensionality of the environment, by comparing the ORs that result from previous experiments [1] and computer simulations [2] of Ag (films or particles) equilibrated on flat Ni substrates, with simulations of a Ag particle embedded within a Ni matrix. In addition, we have performed simulations of certain configurations in which a Ag particle is partially embedded in a Ni substrate in order to investigate the transition from 2-D to 3-D behavior.

In the previous experiments [1], the ORs displayed by a Ag film/particle equilibrated on about 200 different surface orientations of a polycrystalline Ni substrate were determined. The distribution of Ag ORs obtained is shown schematically in the standard stereographic triangle of Fig. 1. On Ni orientations that fall within the (111)-(110)-(210) orange part of the triangle, Ag adopts a cube-on-cube OR (labeled C-C, which may be expressed as  $\text{Ag}\{111\}\langle 110\rangle // \text{Ni}\{111\}\langle 110\rangle$ ), with some fraction of the Ag present in a twin-related orientation to the cube-on-cube orientation. The oct-cube OR (labeled O-C, which may be expressed as  $\text{Ag}\{111\}\langle 110\rangle // \text{Ni}\{100\}\langle 110\rangle$ ) is only observed for Ag equilibrated on Ni(100). The dashed line connecting the (210) to (111) poles, which is the trace of the  $(\bar{1}\bar{2}1)$  plane, represents Ni substrate orientations on which Ag adopts mainly a twin OR with some cube-on-cube OR present (labeled T/C-C). Finally, for Ag on Ni orientations that fall within the (100)-(111)-(210) green portion of the triangle (and labeled S for "special") the OR of Ag undergoes a gradual transition from the oct-cube to the twin/cube-on-cube ORs.

In the simulations [2], which were carried out by molecular dynamics (MD) in conjunction with embedded atom method (EAM) potentials [3], the ORs that developed in Ag films equilibrated on 12 different Ni substrate orientations were found to be in excellent agreement with the experimental results. This provides some confidence that the results of computer simulation based on these EAM potentials are reliable for the Ag/Ni system.

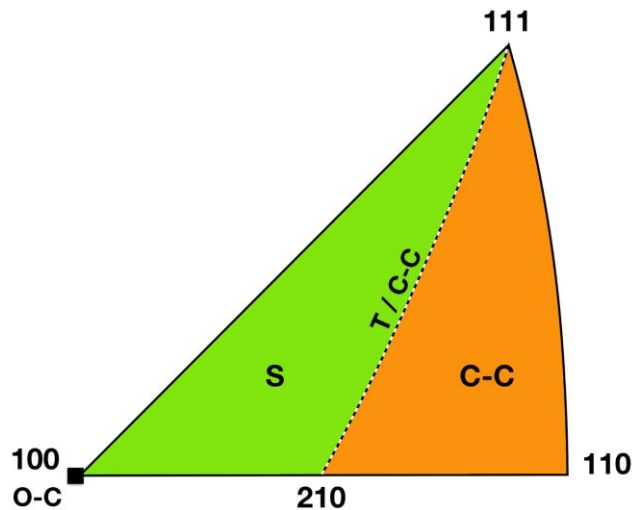


**Fig. 1.** Standard stereographic triangle indicating the ORs displayed by Ag on various Ni substrate orientations (2-D constraints) [1]. The region colored orange and labeled C-C represents Ni substrate orientations on which Ag adopts a cube-on-cube OR, as well as some twin OR. Along the dashed line labeled T/C-C the Ag adopts mainly a twin OR, with some cube-on-cube OR. On the Ni(100) substrate (point labeled O-C) Ag adopts the oct-cube OR. The region colored green and labeled S (for "special") is a region where the Ag OR undergoes a gradual transition O-C to T/C-C (color on line). See text.

As we shall see, the principal crystallographic planes of Ni that are stable in contact with embedded Ag (i.e. under 3-D constraints) are the Ni{111} and Ni{100}. Since Ag{111} coexists with planar Ni{111} in the cube-on-cube OR, whereas it coexists with planar Ni{100} in the oct-cube OR, the question of what happens when a Ag crystal is fully embedded in Ni, where its {111} planes cannot coexist simultaneously with both Ni{111} and Ni{100} surfaces, is worthy of investigation.

The Ni-Ag alloy system represents a convenient model system for the present study. Ni and Ag are almost insoluble in each other in the solid state, and as a result the coexisting solid equilibrium phases consist of essentially pure Ni and Ag at all temperatures. This avoids any concerns regarding the effects of compositional changes on lattice matching of the two phases.

## COMPUTATIONAL APPROACH

### Computational framework

Simulations were performed by molecular dynamics (MD) and/or lattice statics (LS), using the LAMMPS code [4, 5], in conjunction with EAM potentials [3]. These potentials include many body effects, and have been used extensively in previous studies of the Ag-Ni system [6-21]. MD simulations were conducted as follows. A computation cell consisting of Ni and Ag

was heated gradually to 900 K over a period of 200 psec, held at 900 K for a period of 4 nsec in order to approach equilibrium, and then relaxed by LS to remove thermal noise. In most cases it was found that the structure ceased to evolve significantly after equilibration times of 4 nsec at 900 K. If this procedure did not produce satisfactory equilibration, the above cycle was applied several more times, up to total equilibration times of 20 nsec. In a few cases, the temperature to which the computational cell was initially heated was raised to 1250 K, before equilibrating at 900 K.

### 2-D constraints – films on substrates

The results reported here on simulation of ORs of Ag films on flat substrates are taken from a previous study [2]. The initial computational cells consisted of Ni slabs containing between 30,000 to 50,000 atoms, with approximate dimensions of 10 nm in the x- and y-directions, and between 4 and 6 nm in thickness in the z-direction. The x-y Ni surfaces were oriented in preselected (hkl) planes. The Ag films consisted of about 5,000 atoms deposited on the top Ni surface. In order to avoid configurational bias, the Ag atoms of the film were initially arranged randomly, and allowed to crystallize during the MD simulation. Periodic boundary conditions were applied in the x- and y-directions, whereas the z-directions of the Ni slabs and Ag films were terminated by free surfaces.

### 3-D constraints – embedded particles

In order to effect complete 3-D constraints of Ag particles by the Ni matrix, configurations consisting of a Ag particle initially embedded in a spherical cavity of the matrix were employed. The Ni matrix consisted of about 100,000 atoms arranged in the form of a cube, which contained a centrally located Ag particle of about 4000 atoms. 3-D periodic boundary conditions were applied to these computations.

In the case of simulations of Ag particles embedded in a Ni matrix, it was not possible to use an initially random distribution of Ag within the Ni cavity, as the lower density of the randomly distributed Ag would have led to undesirable voids, as a result of shrinkage during MD equilibration. However, in order to avoid bias in the final OR of completely embedded Ag, three different initial configurations were explored. These consisted of (a) an embedded Ag particle in an initially oct-cube OR:  $\text{Ag}(111)[01\bar{1}] // \text{Ni}(100)[01\bar{1}]$ ; (b) an initial OR that corresponded to neither the oct-cube nor the cube-on-cube OR, in which the Ag particle was placed in the Ni matrix after rotation by  $45^\circ$  about the z-axis, thus giving a  $\text{Ag}(001)[100]//\text{Ni}(001)[110]$  OR; and (c) a configuration where the Ag was given a cube-on-cube OR in the Ni matrix. In each case, the Ni cavity was trimmed by gradually removing Ni

atoms that were closer than a prescribed distance from Ag atoms. Each of the resulting configurations was relaxed by lattice statics, and the minimum energy configuration was then used as the initial configuration for further computation.

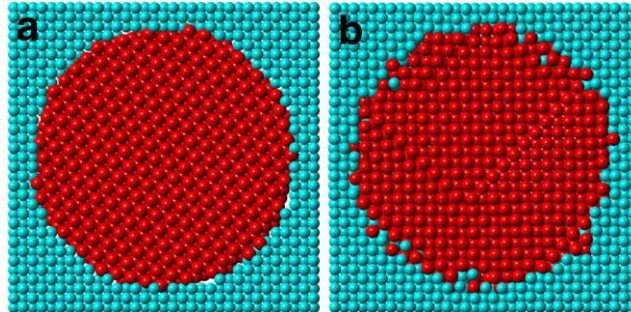
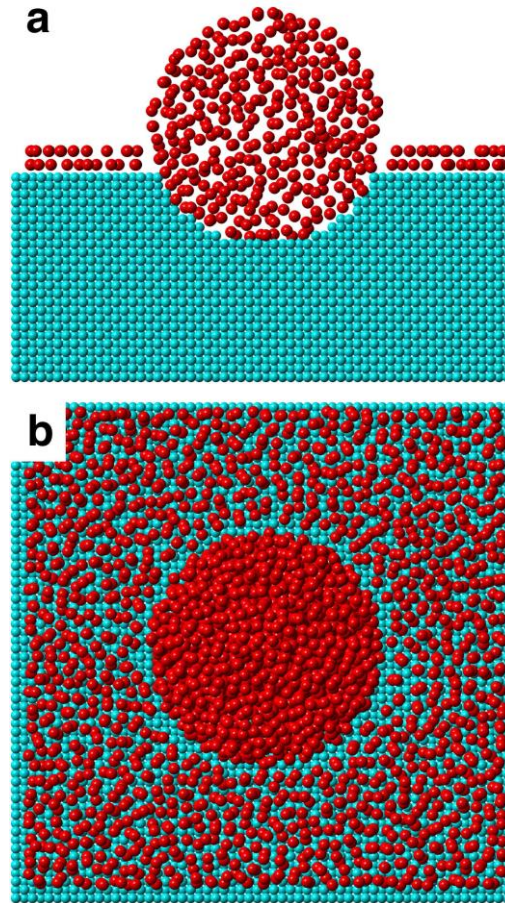


Fig. 2. Structure of an embedded Ag particle in a Ni matrix (Ag atoms red and Ni atoms blue). (a) Slice along a Ni(100) plane through the approximate center of the initial configuration of a Ag particle in an oct-cube OR on the Ni(100) plane, (b) after heating to 1250 K, cooling to 900 K, then holding 4 nsec at 900 K, the particle acquires a cube-on-cube OR.

The three resulting configurations were treated by MD using the following cycle: pre-heating gradually to 1250 K, cooling to 900 K, equilibrating at 900 K for 4 nsec, and finally applying LS so as to remove thermal noise. Although 1250 K lies a few degrees above the melting point of Ag (1235 K) it is quite common for embedded particles to remain solid well above their melting points, as has been shown experimentally for the case of Ag embedded in Ni [22]. No evidence of melting was detected in the present simulations. The final configuration for all three initial ORs was a cube-on-cube OR of Ag in the Ni matrix (as shown in Fig. 2b for the case of the initially oct-cube OR displayed in Fig. 2a) clearly indicating that cube-on-cube was the preferred (i.e. equilibrium) OR. Since the above results established that a cube-on-cube OR is the equilibrium 3-D OR, all further results on embedded Ag particles are reported for computations using an initial cube-on-cube OR.

#### Intermediate constraints – particles in dimples

In order to produce particles with constraints lying between 2-D and complete confinement within a matrix (3-D), simulations were also performed on Ag particles partly embedded in dimpled Ni(100) substrates. The dimple depth was varied as a means of changing the degree of 3-D constraint imposed on the Ag phase. In addition, two dimple shapes were used, spherical dimples as illustrated in Fig. 3, and faceted dimples as shown in Fig. 4.



**Fig. 3.** Example of the initial configuration for the simulation of Ag on a Ni{100} substrate with a spherical dimple; Ag atoms in red, Ni atoms in blue. (a) Slice through center of substrate, (b) top view.

Fig. 3a shows a slice through the center of the initial configuration of a computational cell for the simulation of a Ag particle on a dimpled Ni substrate. The dimple in this Ni(100) substrate is shaped in the form of a spherical segment of radius  $r=7a_{Ni}$ , where  $a_{Ni}$  is the Ni lattice constant. The depth of the dimple shown in Fig. 3 is  $4 a_{Ni}$ . Ag is distributed in two ways: as a randomly arranged sphere of Ag atoms that sits in the dimple, and as randomly located Ag atoms on the planar region of the slab surface; a view of the initial configuration from above is shown in Fig. 3b. When configurations with just the random Ag sphere are used as the initial configuration (i.e. without the added Ag on the planar Ni surface), Ag from the sphere spreads out over the flat Ni surface during MD equilibration to form an adsorbed Ag surface layer that coexists in equilibrium with the 3-D Ag particle in the dimple. Since this diffusive process is slow, placing some Ag initially on the flat part of the Ni substrate allows a reduction of the time taken for equilibration of the Ni surface. Also, by distributing both the

Ag in the dimple and on the planar Ni surface initially in a random manner, any bias on the structure of the Ag that might be inherited from the initial configuration is avoided.

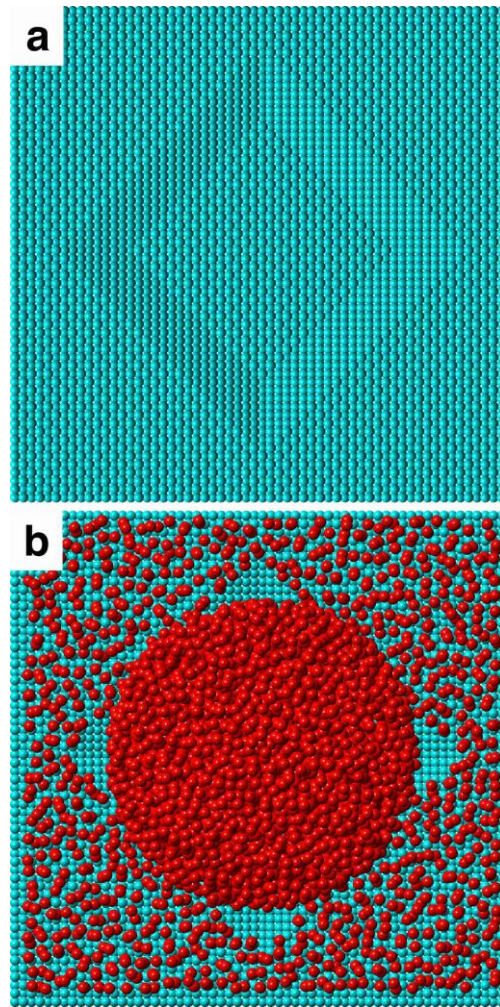


**Fig. 4.** (a) Example of a Ni substrate with a deep faceted dimple. (b) Initial configuration of Ag for the case of a faceted dimple, as viewed from above (cf. Fig. 3b).

Computations have also been performed using dimples with faceted shapes in order to assess the effects of dimple shape on progressive confinement of Ag. The shape of the faceted dimple is shown in Fig. 4a. Dimple depth in Fig. 4a is  $4 a_{Ni}$ . Figure 4b shows the structure of the initial Ag configuration prior to MD simulation; the Ag is randomly distributed in the form of a sphere in the region of the dimple, and as a random layer over the planar substrate, as was the case for the spherical dimple described in Fig. 3.

#### Common neighbor analysis

In addition to the simulations described above, some of the structures resulting from MD and/or LS were subjected to the so-called common neighbor analysis (CNA) [23]. This

type of analysis is able to examine the environment of an atom and determine whether it occupies a site with surroundings that are characteristic of a particular crystal structure. The CNA used here was limited to identifying atoms in sites with surroundings characteristic of FCC, HCP or "unknown" types of sites.

## RESULTS AND DISCUSSION

### 3-D Ag confinement in Ni

We begin by describing the results of simulations of Ag embedded in Ni, where the primary purpose was to gain information on the OR of Ag for the case of complete 3-D confinement. Figure 5 displays 2 views, along a close packed  $\langle 110 \rangle$  direction, of slices through the approximate center of an equilibrated Ag particle embedded in Ni. Figure 5a shows the Ag particle together with the surrounding Ni, whereas Fig. 5b is a view of just the Ag particle, with a color-coding corresponding to a determination of site coordination by CNA. "Unknown" sites in Fig. 5b (colored green) are either sites located on the interface of the particle, which lack a full complement of Ag neighbors and are therefore unidentifiable, or ones located in regions where the local crystalline order has been disturbed by defects of various types.

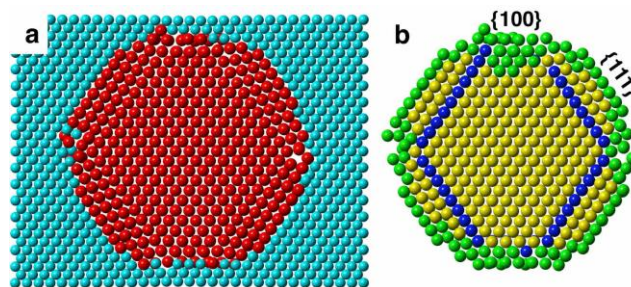


**Fig. 5.** Slices of an embedded Ag particle after equilibration for 4 nsec at 900K, viewed along a  $\langle 110 \rangle$  direction. (a) Slice through the approximate center of the Ag particle and the surrounding Ni matrix (Ag atoms red, and Ni atoms light blue); (b) slice through the Ag particle after applying the common neighbor analysis (atoms in FCC sites yellow, those in HCP sites dark blue, and unknown sites green).

Several features are worthy of note. The Ag particle is bounded primarily by  $\{100\}$  interface planes (top and bottom) and by  $\{111\}$  interface planes (diagonal planes on left and right hand sides of the figure). There may be small  $\{110\}$  interface planes at the junction between the two  $\{111\}$  interface planes on the left and right edges respectively; however these regions appear to be rounded rather than flat, implying that, at the equilibration temperature of 900 K, the  $\{110\}$  interfaces lie above their roughening temperature. Whereas

the core of the Ag particle is clearly aligned with the surrounding Ni crystal (Fig. 5a), indicating a cube-on-cube OR, the regions near the  $\{111\}$  faces display different orientations. In particular, in Fig. 5b, the regions near the  $\{111\}$  faces are seen to be separated from the cube-on-cube core by single  $\{111\}$  planes that display a hexagonal CNA assignment. Such single hexagonally coordinated planes in FCC crystals represent coherent twin grain boundaries.

Finally, it is important to mention that the cube-on-cube OR found by MD is consistent with the OR found experimentally by electron diffraction in TEM, for Ag particles embedded in Ni, prepared by melt spinning of Ni-10%Ag ribbons [22]. Such a cube-on-cube OR has also been observed experimentally for Pb particles equilibrated in Al, a similar low mutual solubility binary system [24] with large lattice mismatch.

### 2-D Ag confinement on Ni substrates

In the previous work mentioned above [1], the behavior of Ag films equilibrated on a large number of Ni substrates of different orientations has been studied. That work showed that the range of observed ORs was quite large, as there is a whole family of "special" ORs which represent a gradual transition from the oct-cube OR on Ni $\{100\}$  to the twin/cube-on-cube ORs displayed along the dashed line labeled T/C-C in Fig. 1. Those results were summarized above in Fig. 1. However, when completely embedded in Ni, Ag displays a single OR, the cube-on-cube OR, as has been demonstrated in the previous section. This 3-D OR is consistent with the OR observed on Ni substrates with orientations lying in the (111)-(110)-(210) orange region of Fig. 1, but coincides neither with the 2-D oct-cube OR of Ag on Ni(100), nor with the family of special ORs. Thus, one important question still needs to be answered: as a Ag crystal is gradually embedded in, say, Ni(100), at what point does it undergo a change from 2-D to 3-D behavior?

### Gradual increase in Ag confinement in Ni

A gradual change in Ag confinement was accomplished by simulations of Ag on dimpled Ni $\{100\}$  substrates. Dimples were either in the shape of a spherical segment, or fully faceted with a  $\{100\}$  bottom and  $\{111\}$  sides, so as to mimic part of the shape of a fully embedded particle such as the example shown in Fig. 5. Dimple depth was gradually increased in order to modify the extent of confinement.

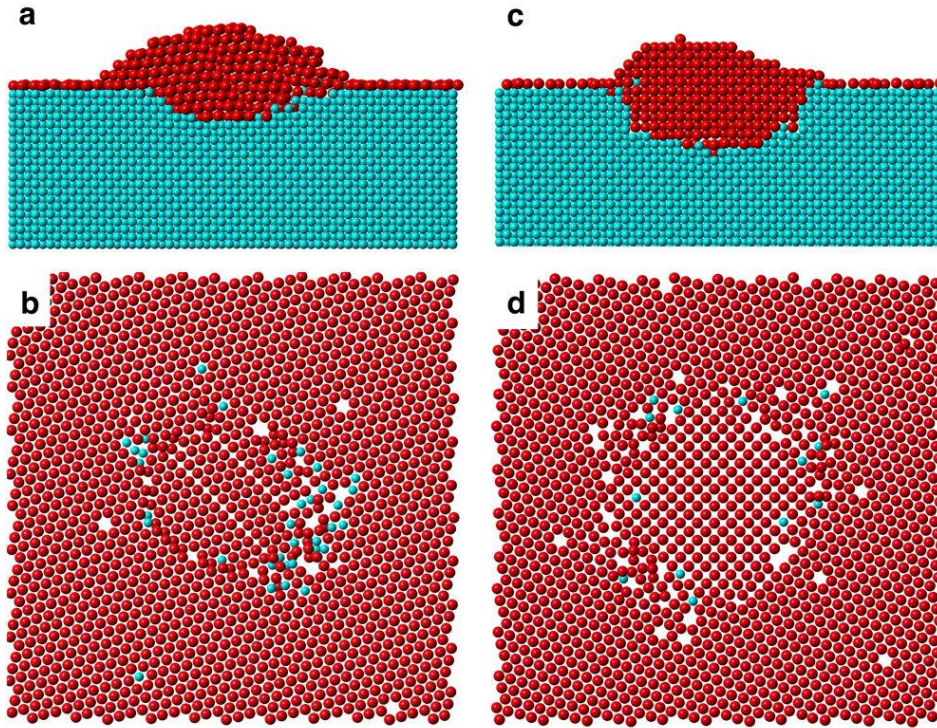


**Fig. 6.** Ag particle on dimpled Ni{100} substrates, after MD equilibration (Ag atoms in red, Ni atoms in blue). Dimple depth was varied from 2 Ni-lattice constants in (a) and (b), to 4 Ni-lattice constants in (c) and (d). (a) and (c) are vertical slices through the center of the dimple, and (b) and (d) are horizontal slices at the level of the Ag adsorption layer on the planar surface of the Ni substrates.

We first describe the results of equilibrating Ag on Ni{100} substrates with dimples in the shape of spherical segments. These dimples were all 7 Ni lattice constants in radius, but varied in depth. Examples of dimples with depths of 2 and 4 Ni lattice constants are shown in Fig. 6. These results were obtained by MD simulations at 900 K of initial configurations similar to those shown earlier in Fig. 2. In the case of the shallow dimple, the structure of Ag can be seen in Fig. 6a to consist of a Ag particle in the dimple and a Ag adsorbed monolayer over the planar part of the substrate. In Fig. 6b, which is a slice at the level of the Ag adsorbed monolayer, both the adsorbed Ag as well as the Ag in the dimple can be seen to have a hexagonal symmetry on the Ni{100} substrate (with the exception of an occasional fault) as expected for an oct-cube OR. In contrast, in Fig. 6d for the case of the deeper dimple, there is a clear difference in structure between the hexagonal adsorbed Ag monolayer and the portion of the Ag slice through the Ag particle in the dimple, which displays a square symmetry consistent with a cube-on-cube OR for the portion of Ag in the dimple. Thus, the OR of the partially constrained particle undergoes a transition from oct-cube when equilibrated in a shallow dimple to a cube-on-cube OR when equilibrated in a deeper dimple. This transition takes place for a dimple depth lying between 2 and 4 Ni lattice constants.

Since the oct-cube OR is strongly dependent on Ag equilibration with Ni{100} surfaces it was considered important to determine whether simulations performed on fully faceted dimples, with well-defined {100} planes, would also show the transition from oct-cube to cube-on-cube at a dimple depth similar to the case of spherically-shaped dimples. Results of those simulations are summarized in Fig. 7.

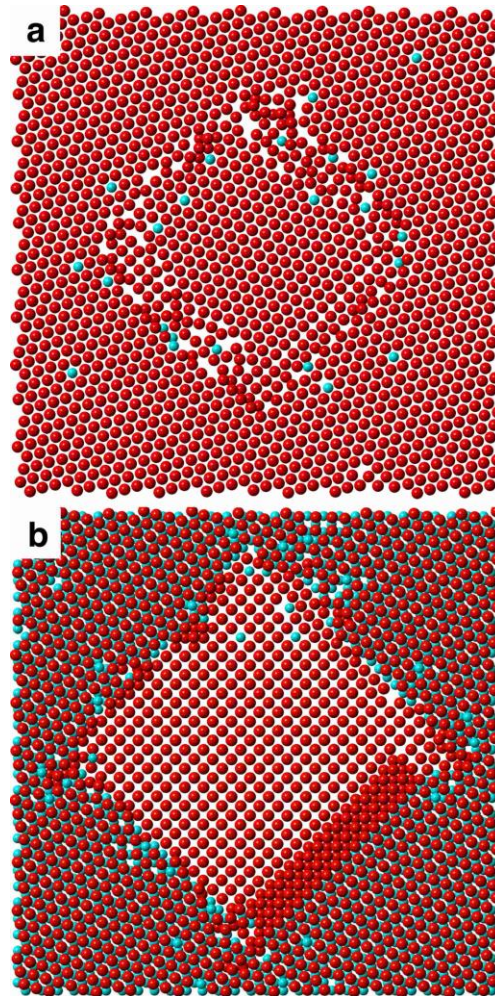


**Fig. 7.** Horizontal slices at the level of the adsorbed Ag monolayer on a planar Ni{100} surface after MD equilibration at 900 K. (a) Ag equilibrated on substrate with a dimple depth of 2 Ni-lattice constants, and (b) Ag equilibrated on a substrate with a dimple depth of 4 Ni-lattice constants. (Ag atoms in red, Ni atoms in blue).

The shapes of a faceted dimple, and of the initial Ag configuration in such a dimple were shown earlier in Fig. 4. The results of MD simulation on a substrate with a dimple having a bottom {100} facet of about 12 Ni lattice constants on a side and a depth of 2 Ni-lattice constants are shown in Fig. 7a. The figure shows a slice through the dimple at the level of the adsorbed Ag monolayer on the planar part of the Ni substrate. The Ag displays a hexagonal

symmetry in both the adsorbed layer and in the portion of the Ag particle residing in the dimple, as is consistent with an oct-cube OR. Figure 7b shows that for a substrate with a dimple of 4 Ni-lattice constants in depth (and the same size bottom facet) the Ag over the dimple has adopted a square symmetry characteristic of a cube-on-cube OR. These results are essentially the same as those obtained on substrates with spherical dimples, and confirm that a transition in OR from oct-cube to cube-on-cube occurs for dimple depths of between 2 and 4 Ni lattice constants. However, it should be emphasized that the depth of the dimple at the transition from oct-cube to cube-on-cube OR depends on the ratio of the area of the bottom  $\{100\}$  facet to that of the lateral  $\{111\}$  facets, as discussed in more detail in the appendix.

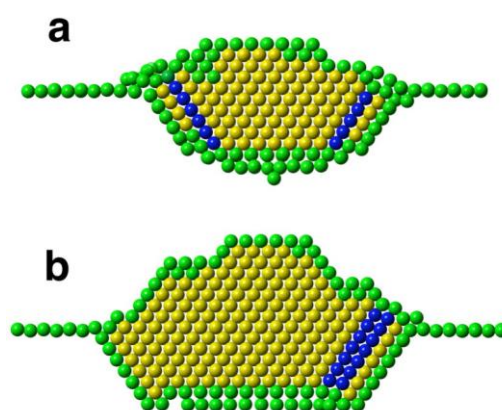


**Fig. 8.** Results of CNA on slices through Ag particles viewed along a  $\langle 110 \rangle$  direction, with atoms in FCC sites colored yellow, those in HCP sites in dark blue, and sites with unknown coordination in green. (a) Particle in a  $4a_{\text{Ni}}$  deep dimple in the shape of a spherical segment, (b) particle in a  $4a_{\text{Ni}}$  deep faceted dimple.

It is also interesting to investigate the defects that are present in partially embedded Ag, as determined by CNA, after simulation by MD. Figure 8 shows the results of CNA performed on Ag residing on Ni $\{001\}$  substrates with dimples either in the shape of spherical segments (Fig. 8a) or entirely faceted (Fig. 8b). The particle in Fig. 8a displays one layer of atoms with hexagonal coordination (colored blue) in the vicinity of both of its visible  $\{111\}$  edges, much like the completely embedded Ag particle of Fig. 5b. As mentioned earlier, a single  $\{111\}$  plane of atoms with hexagonal coordination is the signature of a coherent twin grain boundary. The Ag particle in the faceted dimple (Fig. 8b) displays two adjacent  $\{111\}$  planes with hexagonal coordination in the vicinity of only one of its visible  $\{111\}$  edges. The double  $\{111\}$  hexagonal layer is the signature of an intrinsic stacking fault. The CNA results

shown here are, however, not unique, in the sense that different computations performed from the same starting configuration, but using different seeds for the random number generator used in the simulations, could produce different defect structures. However, coherent twin grain boundaries were the most common type of planar defects observed to occur near the  $\{111\}$  interfaces of Ag particles during these simulations.

## CONCLUSIONS

Comparison of the results of simulations in which Ag was equilibrated on 2-D Ni substrates with those of simulations in which Ag was embedded in Ni (3-D confinement) showed the following differences. Whereas equilibration of Ag embedded in Ni produces a single equilibrium OR, specifically a cube-on-cube OR, equilibration of Ag on flat Ni substrates (i.e. 2-D confinement) produces a series of ORs, as was shown in our previous experiments [1]. This is an important observation, as it runs contrary to conventional wisdom, which supposes that the ORs displayed in the presence of 3-D confinement (e.g. during phase transformations) will also tend to be displayed in epitaxy on a substrate. Thus, one important conclusion from this work is that ORs produced by 3-D confinement do not provide an appropriate basis for inferring the ORs that arise when films are deposited and equilibrated on planar substrates.

It has also been shown that by progressively increasing the degree of 3-D confinement of Ag particles, through an increase in the depth of dimples at the surface of Ni $\{100\}$  substrates, it is possible to produce a transition from an oct-cube OR for Ag equilibrated in shallower dimples, to a cube-on-cube OR for Ag in deeper dimples. The specific details of the depth at which the transition occurs are sensitive to the interfacial energies of the dimple.

## Acknowledgments

PW wishes to acknowledge use of the computational resources of the National Energy Research Scientific Computing Center, which is supported by the Office of Science of the U.S. Department of Energy under Contract No. DE-AC02-05CH11231. DC wishes to thank the Agence Nationale de la Recherche for support of her research under grant ANR-GIBBS-15-CE30-0016. In addition, the authors wish to thank Prof. N. Bozzolo for useful discussions.

## Conflicts of Interest

The authors declare that they have no conflicts of interest.

## References

- [1] Chatain D, Wynblatt P, Rollett AD, Rohrer GS (2015) Importance of interfacial step alignment in hetero-epitaxy and orientation relationships: the case of Ag equilibrated on Ni substrates. Part 2 experiments. *J Mater. Sci.* 50:5276-5285.
- [2] Wynblatt P, Chatain D (2015) Importance of interfacial step alignment in hetero-epitaxy and orientation relationships: the case of Ag equilibrated on Ni substrates. Part 1 computer simulations. *J Mater. Sci.* 50:5262-5275.
- [3] Plimpton SJ (1995) Fast parallel algorithms for short-range molecular dynamics, *J Comp Phys* 117:1-19.
- [4] <http://www.cs.sandia.gov/~sjplimp/lammps.html> Accessed 2 May 2015
- [5] Foiles SM, Baskes MI, Daw MS (1986) Embedded-atom-method functions for the fcc metals Cu, Ag, Au, Ni, Pd, Pt, and their alloys, *Phys Rev B* 33:7983.
- [6] Dregia SA, Bauer CL, Wynblatt P (1986) The structure and composition of interphase boundaries in Ni/Ag-(001) thin films doped with Au, *Mater Res Soc Symp Proc* 56:189-194.
- [7] Dregia SA, Wynblatt P, Bauer CL (1987) Epitaxy for weakly interacting systems of large misfit, *Mater Res Soc Symp Proc* 94:111-120.
- [8] Dregia SA, Wynblatt P, Bauer CL (1989) Computer simulations of epitaxial interfaces, *Mater Res Soc Symp Proc* 141:399-404.
- [9] Gao Y, Dregia SA, Shewmon PG (1989) Energy and structure of (001) twist interphase boundaries in the Ag/Ni system, *Acta Metall* 37:1627-1636.
- [10] Gao Y, Shewmon PG, Dregia SA (1989) Investigation of low-energy interphase boundaries in Ag/Ni by computer simulation and crystallite rotation, *Acta Metall* 37:3165-3175.
- [11] Maurer R, Fischmeister HF (1989) Low energy heterophase boundaries in the system silver/nickel and in other weakly bonded systems, *Acta Metall* 37:1177-1189.
- [12] Gao Y, Merkle KL (1990) Atomic Structure of Ag/Ni interfaces, *Mater Res Soc Symp Proc* 183:39-44.
- [13] Gao Y, Merkle KL (1990) High-resolution electron microscopy of metal/metal and metal/metal-oxide interfaces in the Ag/Ni and Au/Ni systems, *J Mater Res* 5:1995-2003.
- [14] Gumbsch P, Daw MS, Foiles SM, Fischmeister HF (1991) Accommodation of the lattice mismatch in a Ag/Ni heterophase boundary, *Phys Rev B* 43:13833.
- [15] Gumbsch P (1992) Atomistic study of misfit accommodation in cube-on-cube oriented Ag/Ni heterophase boundaries, *Z Metallkd* 83:500-507.
- [16] Allameh SM, Dregia SA, Shewmon PG (1994) Structure and energy of (110) twist boundaries in the Ag/Ni system, *Acta Metall Mater* 42:3569-3576.
- [17] Allameh SM, Dregia SA, Shewmon PG (1996) Energy of (110) twist boundaries in Ag/Ni and its variation with induced strain, *Acta Mater* 44:2309-2316.

- [18] Floro JA, Thompson CV, Carel R, Bristowe PD (1994) Competition between strain and interface energy during epitaxial grain growth in Ag films on Ni(001), *J Mater Res* 9:2411-2424.
- [19] Gumbsch P (1997) The accommodation of lattice mismatch in Ag/Ni heterophase boundaries, *J Phase Equilibria* 18:556-561.
- [20] Mroz S, Jankowski Z, Nowicki M (2000) Growth and isothermal desorption of ultrathin silver layers on the Ni(111) face at the substrate temperature from 180 to 900 K, *Surface Sci* 454:702-706.
- [21] Chambon C, Creuze J, Coati A, Sauvage-Simkin M, Garreau Y (2009) Tilted and nontilted Ag overlayer on a Ni(111) substrate: structure and energetics, *Phys Rev B* 79:125412, and references therein.
- [22] Zhong J, Zhang LH, Jin ZH, Sui ML, Lu K (2001) Superheating of Ag nanoparticles embedded in Ni matrix, *Acta Mater* 49:2897–2904.
- [23] Faken D, Jonsson H (1994) Systematic analysis of local atomic structure combined with 3D computer graphics, *Computational Materials Science* 2:279-286.
- [24] Dahmen U, Xiao SQ, Paciornik S, Johnson E, Johansen A (1997) Magic-Size Equilibrium Shapes of Nanoscale Pb Inclusions in Al , *Phys Rev Lett* 78:471-474, and refs therein.

## Appendix

As a first approximation, we take the total excess energy of a Ag particle in a faceted dimple substrate to be the sum of the energies of all its interfaces multiplied by their areas. For the purpose of these estimates we shall use the energies of the Ni/Ag interfaces computed by Gao et al. [10], using the same EAM potentials as those used in the present MD simulations. Those are listed in Table 1.

Table 1. Calculated Ni/Ag interfacial energies (mJ/m<sup>2</sup>) [10]

	Ag{100}	Ag{110}	Ag{111}
Ni{100}	814	1124	437
Ni{110}	995	828	988
Ni{111}	670	960	416

Let us begin by comparing the energies of the bottom Ni{100} dimple interface for the cases of an oct-cube vs. a cube-on-cube OR. The energy of the oct-cube Ni{100}/Ag{111} interface is 437 mJ/m<sup>2</sup>, and for the cube-on-cube Ni{100}/Ag{100} it is 814 mJ/m<sup>2</sup>. Thus, the dimple bottom interface has a clear energy advantage in the oct-cube vs. the cube-on-cube comparison. As the depth of the dimple increases, a progressively larger fraction of the interface will consist of Ni{111} facets. In the case of the cube-on-cube OR the resulting four Ni{111}/Ag{111} interfaces have the lowest energy, namely: 416 mJ/m<sup>2</sup>. This is consistent with the expectation that {111}/{111} interfaces in FCC metals will tend to have the lowest interfacial energy.

In the case of the oct-cube OR, the Ag side of the four Ni{111} interfaces are all different: they consist of Ag {100} and {221} planes as well as two other high index planes. Of these interfaces, only the energy of the Ni{111}/Ag{100} is known to be 670 mJ/m<sup>2</sup>. The average of all the interfacial energies computed by Gao et al. [10] is about 800 mJ/m<sup>2</sup>. Considering this figure to be a reasonable estimate of the average energy of the Ni{111}/Ag{hkl} interfaces, it is clear that a transition in stability from oct-cube to cube-on-cube OR will occur when the area of Ni{111} will exceed Ni{100} area at the Ni/Ag interface, i.e. somewhere between a dimple depth of  $2a_{Ni}$  and  $4a_{Ni}$ .

It is worth noting that the contribution of strain energy to the total excess energies of the two configurations may also contribute to the transition.